Finite single wall capped carbon nanotubes under hydrostatic pressure

2006 J. Phys.: Condens. Matter 18 9119

(http://iopscience.iop.org/0953-8984/18/39/037)

INSTITUTE OF PHYSICS PUBLISHING JOURNAL OF PHYSICS: CONDENSED MATTER

J. Phys.: Condens. Matter **18** (2006) 9119–9128 doi:10.1088/0953-8984/18/39/037

Finite single wall capped carbon nanotubes under hydrostatic pressure

S E Baltazar[1], A H Romero[2], J L Rodríguez-López[1] and R Martoňák[3]

[1] IPICYT, Advanced Materials Department, Camino Presa San José 2055, 78216 San Luis Potosí, SLP, México
[2] CINVESTAV, Unidad Querétaro, Libramiento Norponiente No. 2000 Real de Juriquilla, 76230 Querétaro, Qro., México
[3] Computational Science, Department of Chemistry and Applied Biosciences, ETH Zurich, USI Campus, Via Giuseppe Buffi 13, CH-6900 Lugano, Switzerland

E-mail: aromero@qro.cinvestav.mx

Received 7 June 2006, in final form 24 August 2006
Published 15 September 2006
Online at stacks.iop.org/JPhysCM/18/9119

Abstract

We report a classical molecular dynamics isothermal–isobaric ensemble (*NPT*) implementation for the simulation of pressure effects on finite systems. The method is based on calculating the enclosed surface area by means of the Delauney triangulation method, which results in a fairly accurate description of the surface and the system volume. The external pressure is applied to the system by external forces acting on the triangulated surface covering the nanostructure. Pressure is exerted perpendicularly to every one of the Delauney triangles, by equally distributing the force to every corner of a triangle. We applied the method to finite single wall capped carbon nanotubes (SWCNTs) with different chiralities and different tube lengths ranging from 4 nm up to 30 nm. Pressure effects are studied as a function of the radii and the nanotube length, as well as as a function of temperature. Our results are in very good agreement when compared with both experimental and other theoretical results.

(Some figures in this article are in colour only in the electronic version)

1. Introduction

The study of finite systems such as nanocrystals, fullerenes, clusters and molecular systems possesses important implications in biology [1], electronics [2], medicine [3], etc. It is well established nowadays that structural changes due to external forces, like tensile strain or hydrostatic pressure, can radically change the electrical and mechanical properties of these structures. In particular, for carbon nanotubes, Cao and coworkers [4] have measured the electromechanical properties of suspended SWCNTs under stretching. From this study, they suggest that quasi-metallic SWNTs are potentially useful for highly sensitive electromechanical

sensors (strain gauges, pressure sensors, etc). Also, exceptionally large reversible volume reduction upon high pressures in rope bundles of CNTs [5] reveals high storage of mechanical energy that future designs of energy-absorbing nanocomposite materials could take advantage of. This observation on these type of materials can also be extrapolated to other finite systems, where external forces produce changes on some properties of the system, leading to a completely new behaviour. This pursuing of new properties is one of the *leitmotifs* behind nanostructured materials science.

Considering systems under pressure, a large amount of studies at both classical and *ab initio* levels has been devoted to periodic systems since the introduction of molecular dynamics (MD) simulations in *NPT* ensembles [6, 7]. In these cases, the periodic cell volume is allowed to fluctuate in order to balance the applied pressure. In contrast, there have been just a few studies of finite systems under pressure due to the lack of periodic boundary conditions. In this respect, there have been some approaches to simulate an applied external pressure on finite systems. For example, small to medium size silicon nanocrystals have been studied by using a pressure-transmitting liquid [8–10]. Also, a finite hcp crystal was studied by considering a spherical approximation of the volume [11]. Nanocrystals were also studied by applying a volume definition based on atomic volumes [12] and a surface triangulation method was applied to study metallic clusters [13, 14]. In simulations of finite systems under external pressure, the volume of the structures becomes very important and so the most realistic calculation of volume is essential and an appropriate definition is necessary [15].

In this work, we focus on pressure applied to single wall carbon nanotubes. Since the first studies of carbon nanotubes [16], several theoretical and experimental studies about their mechanical [17–20], electrical [4, 21, 22], and optical properties [23, 24] have been reported. The possibility of using them in technological applications has inspired a large amount of studies characterizing their intriguing electronic behaviour and their possible manipulation with external forces [4]. The success of these applications depends on several factors, like nanotube quality, chirality, and how an external force can affect its properties by changing its shape from the cylindrical configuration [17].

By following the recent literature on carbon nanotubes and their response to elastic deformations or application of pressure, one realizes that there is not yet an agreement on the elastic changes produced by pressure on crystalline single walled nanotubes. For example, Elliot *et al* [25] and Tang *et al* [19] have found that *bundle cross-sections*, with a hexagonal structure, can transform to a polygonal phase when hydrostatic pressure is applied, while Chan *et al* [26] find that the hexagonal microstructure is only metastable and the lowest energy state should be an ellipsoid, similar to the result found by Sluiter *et al* for bundles of carbon nanotubes [27]. It is important to mention that elastic models predict for this case that the cross-section should be hexagonal [28]. This observation clearly contradicts the conclusion of Zang *et al* [29], who reported agreement between atomistic models and elastic theories. Even though there are some publications indicating a consensus [30], this is not a general outcome, which points to the need for further studies comparing and contrasting these two methods. The different results obtained from continuum mechanical theory and atomistic theory have been addressed by many authors [30, 31], a point that is stressed by Harik's statement: *The theory of shells may serve as a useful guide, but its relevance for a covalent-bonded system of only a few atoms in diameter is far from obvious* [31]. There is also a very recent discussion based on detailed atomistic calculations of some of the difficulties in applying continuum mechanics concepts to nanotubes [32].

The goal in this paper is to simulate the action of external pressure on finite single-wall capped carbon nanotubes (SWCNTs). The simulation method used is aimed at modelling the effect of an average pressure on a finite nanostructure. The carbon–carbon interactions in

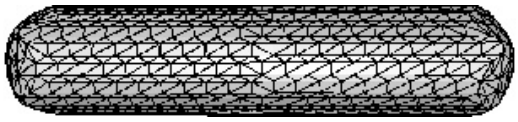

Figure 1. The surface of a (10, 10) finite SWCNT (6 nm in length, 1020 carbon atoms) obtained from the triangulation surface method. The volume is calculated from the Gauss theorem.

the nanotubes are described by an empirical potential derived by Tersoff and Brenner from first principles calculations [33] and adapted by Maruyama [34]. We have considered finite SWCNTs with different chiralities and different lengths ranging from 4 to 30 nm. Another parameter changed in this work is the temperature, which affects the mechanical behaviour of the nanotube. Our results are contrasted with those from Capaz *et al* [35], who implemented the pressure-reservoir method initially proposed by Martoňák *et al* [8] (MMP method), but using an extended Tersoff–Brenner interatomic potential. As a second check for our method, we also implemented the MMP method and calculated the pressure effects just in selected points with the same force field we used in our method. In general, the results presented below agree well with both the Capaz implementation and our own one.

In the next section we describe briefly the basic ideas of our approach and how the pressure is applied, with some details about the simulations. In section 3 we present the results. Finally, in section 4 we present our discussion and conclusions.

2. Simulation method

The method presented in this paper is similar in spirit to the pressure-reservoir method proposed by Martoňák *et al* [8], in which liquid particles interact mainly with surface atoms through short-ranged forces. In our case, the pressure acts only on particles on the surface, but instead of a real pressure-transmitting medium, a suitably defined external force is used.

We start with a triangulated surface calculated on a capped carbon nanotube. The surface is obtained by following the quick-hull algorithm described in [36], with which the minimal polyhedron enclosing a given structure can be obtained (see some applications for metallic clusters in [13, 14]). Even though this algorithm is implemented on surfaces without any concavity, the method can be generalized by relaxing some of the searching parameters, introducing an error parameter which leads to a tighter triangulated surface, as in [37].

Since in our case all atoms are on the surface, the triangulation is performed only at the beginning of the simulation. In principle, it can be recalculated at any point during the simulation if necessary. An example of the output of the algorithm is presented in figure 1 for a capped single wall carbon nanotube. After the triangulation has been performed, the external pressure P is applied to the system as follows: taking a triangle (and its three vertices), the area A_m is calculated. The force applied on each plane is defined as $\vec{f}_m^{\,\mathrm{ext}} = -PA_m\hat{n}$, where A_m and $\hat{n}$ are the area and the normal vector associated to each triangular face. Subsequently, the force is proportionally distributed on the atoms (vertices) related to that triangle. Equations of motion are obtained by adding this external force to the atomic interactions:

$$m_i \frac{\partial^2 r_{i,\alpha}}{\partial t^2} = F_{i,\alpha} + F_{i,\alpha}^{\mathrm{ext}} \qquad \alpha = x, y, z; \quad i = 1, \ldots, N \tag{1}$$

where N is the number of atoms on the surface, which is equal to the number of vertices of the triangulation and $F_{i,\alpha}^{\mathrm{ext}}$ is the distributed force from the applied pressure.

In our simulations, the nanotubes were first thermalized at zero pressure and at a given temperature (usually 50 K), and then the pressure was slowly increased up to 5 GPa in the case

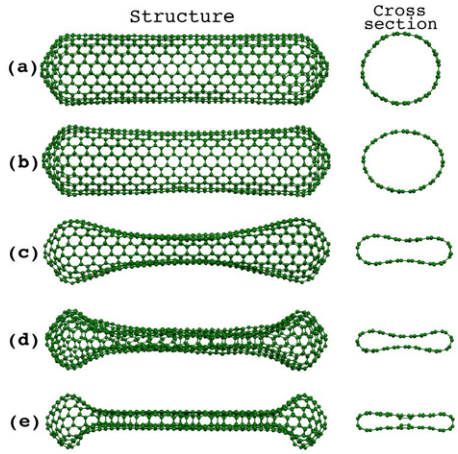

Figure 2. Snapshots at different pressures of a (10, 10) armchair nanotube, 60 Å long, consisting of 1020 atoms and at a temperature of 50 K. In (a) we obtain a cylindrical structure by applying 0.2 GPa, in (b) the shape is ellipsoidal at 1.1 GPa and for (c), (d) and (e) a peanut-shape structure is obtained for 1.2, 3.0 and 6.0 GPa respectively. Notice that, as the pressure is increased, the nanotube has less freedom to vibrate along the radial direction, and at some specific pressure, the system prefers to bend.

of the (5, 5) tube, and up to 2 GPa in the case of the (10, 10) tube. During the time where the pressure was kept constant, the temperature was maintained at the prescribed value by rescaling the velocity every 20 fs until the thermal equilibrium was reached, at which point the rescaling was stopped. After the equilibration was reached, the dynamical evolution was continued for 10/40 ps with a time step of 0.5 fs to perform the measurements. Other simulation parameters were exactly the same as the ones discussed in a previous publication [15].

3. Results

We applied the MD implementation discussed above to capped single wall carbon nanotubes. Since we are dealing with finite systems and we are interested in studying finite size effects, we considered throughout all our calculations two different nanotube lengths. According to the notation introduced by Harik [31], a nanotube is short or long if its aspect ratio, *Diameter* (D)/*Length* (L), is greater or less than 0.1, respectively. To study the case of long nanotubes (with aspect ratios much less than 0.1) we simulated tubes with length 28.8 nm for (10, 10) and 14.1 nm for (5, 5) configurations with aspect ratio of 0.047 and 0.048 respectively. For the short case, we have considered a length of 5.3 nm (aspect ratio 0.256) for the (10, 10) case and 4.5 nm (0.151) for the (5, 5) case. The change in nanotube length helps us to rationalize some of our observations and check possible dependences on this physical parameter.

Molecular dynamics simulations were performed by using a classical semiempirical potential derived from first principles calculations, also known as the Tersoff and Brenner potential [33], with corrections introduced by Yamaguchi and Maruyama [34]. To check our findings, we compared some of our results with the ones obtained from classical MD simulations using the MMP method, as reported by Capaz *et al* [35] and a similar simulation implemented by ourselves. We start our discussion with the case of a short nanotube (10, 10). Figure 2 presents several snapshots of the nanotube at different values of the applied pressure and at a temperature of 50 K. Here, both the axial section and the cross-section are

shown, in the order of increasing pressure from top to bottom. At 0.2 GPa, (a), the nanotube in average preserves a cylindrical structure, in which the only change is a shortening of the C–C bond distance as well as a reduction of the amplitude of radial vibrations such as the breathing mode. At 1.1 GPa, (b), the nanotube becomes elliptical and develops a large curvature along its axis. The caps remain rather rigid and there is only a small decrease of the C–C distance. On average, its principal structural shape remains similar to that at low pressures. At 1.2 GPa, (c), and 3.0 GPa, (d), a transition to a peanut structure is observed as has been reported previously by some authors [25, 29, 35]. At 6.0 GPa, (d), the pressure is rather large and the nanotube is approaching a very elongated structure, in which two planes interact. After a further slight increase of the pressure, the nanotube breaks down. This elastic behaviour is generally observed in all kinds of simulated nanotubes (shorter or longer); the only major difference is in the transition pressure value. It is noteworthy that beyond 3.0 GPa we observe a rocking mode, i.e., the nanotube exhibits a torsion around its principal axis before the cross-section becomes planar. This mode cannot be observed in the case of infinite nanotubes (with periodic boundary conditions) [29, 35]. This vibrational mode could be observed experimentally, for example by Raman spectroscopy, if the nanotube under pressure is free at both ends as in our finite systems.

Upon increasing the applied hydrostatic pressure, SWCNTs are able to excite different radial or axial vibrational modes that are responsible for the observed structural transitions. This can be concluded by analysing the velocity autocorrelation function (VACF). Some of the vibrational peaks appearing at low pressures disappear as the pressure is increased. This observation is consistent with recent experimental results, in which shifts of the radial modes for SWCNT bundles were observed as the pressure was applied [18, 39]. In those experimental works, bundles of nanotubes were immersed in a gasketed diamond anvil cell filled with methanol–ethanol as a pressure transmitting medium. To study the behaviour of the radial breathing mode frequency, ω_{R}, as a function of the nanotube diameter, Venkateswaran *et al* [40] were able to fit the experimental data with a functional form obtained from a simple elastic model. Beyond the transition pressure, when the nanotubes have transformed to have a noncircular cross-section, the breathing mode has changed its symmetry and other vibrational modes become more important. These modes can provoke abrupt transitions by combining their effects (increasing or changing anisotropically the atomic mean square amplitude in different directions and disrupting carbon–carbon bonds). Even though identifying vibrational modes from a velocity autocorrelation function (VACF) analysis could be difficult, we were able to assign the breathing mode for very low pressures and we did obtain an inverse of the diameter dependence of the frequency as reported in [18]. An accurate description of the vibrational modes could be found from the force constants obtained from a static calculation.

The behaviour of the vibrational modes across the transition has been also analysed by calculating the VACF. We considered just three cases: 0.0, 0.6 and 1.2 GPa for (10, 10) tubes and 0.0, 4.0 and 10.0 GPa for (5, 5), and analysed the main peaks observed for each case. These results showed that before the transition which is located at 1.2 GPa for (10, 10) and at 8 GPa for (5, 5) tubes, peaks at values close to the experimental radial breathing and axial modes were found. After the structural transition, those peaks related to the circle–oval cross-section are reduced or suppressed for both (5, 5) and (10, 10) tubes. Moreover, frequency peaks in the power spectra are tube diameter dependent, particularly the radial breathing mode (RBM) ω_{R} that has been calculated for (6, 0), (5, 5), (15, 0), (10, 10) and (20, 0) tubes. We have found that the RBM decreases with the diameter following a D^{-1} dependence, which is the same behaviour reported in [40, 41].

This kind of structural changes was studied by Raman spectroscopy techniques reported by Venkateswaran *et al* [18]. They examined the pressure dependence of the radial and tangential vibrational modes and observed that the radial mode intensity decreases beyond 1.5 GPa for

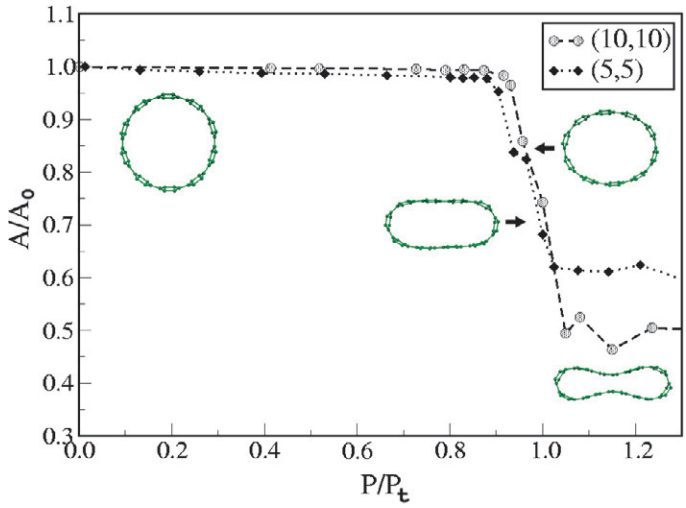

Figure 3. Cross-sectional area as a function of pressure for capped (5, 5) and (10, 10) nanotubes. Statistics were collected and averaged during 10 ps, after thermodynamic equilibrium was reached. Here, pressure has been normalized to the transition pressure (see text).

diameters associated with (10, 10) nanotubes, suggesting that the system undergoes a phase transformation. Also, Peters *et al* [38], based on Raman shifts, have determined a structural phase transition at 1.7 GPa for nanotubes with an average diameter of 13.5 Å. Chesnokov *et al* [5] have also reported changes from cylindrical to ellipsoid shape, which agrees with our calculation.

Chesnokov *et al* also found that nanotubes still undergo reversible deformations up to the transition pressure. It is important to note that the majority of experiments have been performed on nanotubes bundles in which confinement affects the transition pressure. Figure 3 shows the behaviour of the normalized cross-sectional area (A/A_0) for long (5, 5) and (10, 10) nanotubes as a function of the reduced pressure (P/P_t) at a temperature of 100 K. The reduced pressure is calculated by dividing the pressure P by the transition pressure (P_t) defined as the pressure at the maximum value of the slope of the A versus P curve. Upon increase of pressure, we can clearly distinguish two different regimes. At low pressures we observe a slow compression which corresponds to the gradual change from circular (area A_0, $P = 0$) to an oval shape. In this regime we also observed fluctuations between the circular and the oval shape. This shows that the sharp transition from the circular to the oval shape, as suggested from $T = 0$ calculations by Zang *et al* [29], does not exist at finite temperature. Upon further increase of pressure we observe an abrupt drop at P_t where the shape rapidly changes from oval to peanut (area A_1). From figure 3 we can see that this behaviour is the same for different nanotubes, which indicates that the scenario of the structural change is independent of nanotube diameter. However, we have verified that the ratio A_1/A_0 is different for the two tubes. These results are in agreement with the collapse transition of Capaz *et al* [35] and the loading curves shown by Elliott *et al* [25]. On the other hand our results differ from those of Zang *et al* [29] since we find that at finite temperature the oval shape of the cross-section is neither unique nor stable.

In order to systematically study the temperature effect on the pressure-induced structural transitions, we chose to focus on the case of short nanotubes for both studied chiralities. Simulations were performed at several temperatures: 50, 100, 200, 300 K for a (5, 5) nanotube and 50, 100, 200, 400 K for a (10, 10) nanotube. The results are shown in figure 4. In

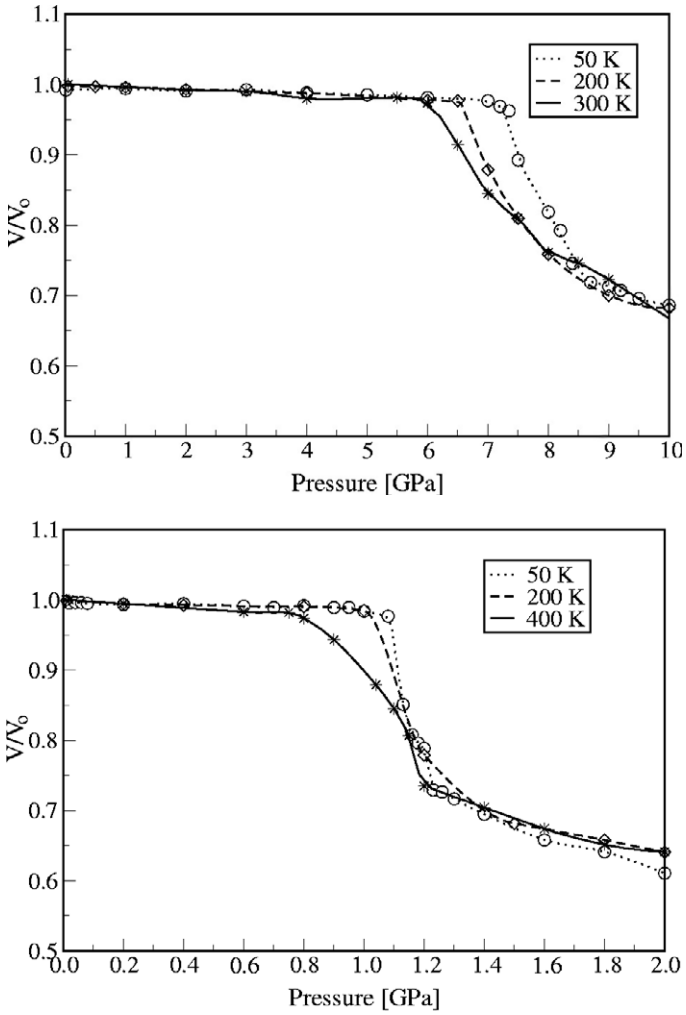

Figure 4. Volume as a function of applied pressure at different temperatures for a (5, 5) nanotube (370 atoms) of length of 42 Å (upper panel) and for a (10, 10) nanotube (920 atoms) of length of 53 Å (lower panel).

general, with increasing temperature the abrupt structural transition from circular to a flattened cross-section becomes broader and more smooth. Similar effects are also found in the case of longer tubes, which indicates that the temperature effects are rather independent of the nanotube length.

Finally, we studied the transition pressure as a function of the tube diameter. This dependence can already be seen in figure 4 and is of great practical importance as it may have a great impact in the design of electromechanical sensors (pressure sensors) or mechanical energy storage devices using carbon nanotubes. If the devices contain mixtures of carbon nanotubes with different diameters, the response to pressure can be obscured by a combination of different elastic deformations of the nanotubes. In figure 5 we show the transition pressure as a function of the tube diameter as obtained for the longest considered nanotubes. The transition pressure decays rather quickly and beyond a diameter of 12 Å it becomes very small. For

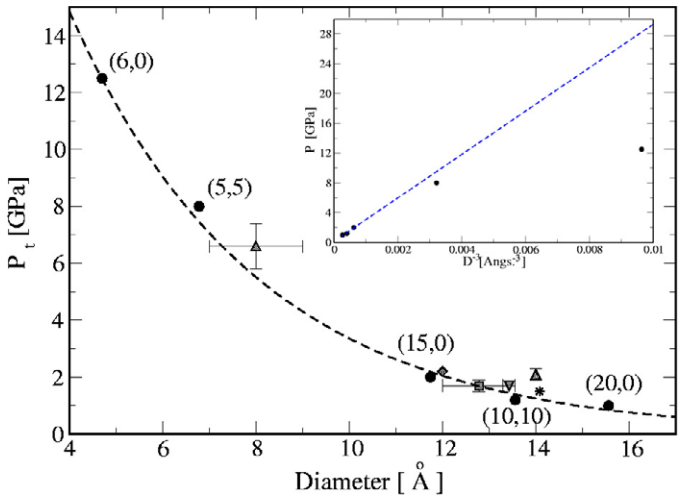

Figure 5. Transition pressure as a function of the tube diameter, D. The dashed line is a guide line through our calculated circular points (see text for details). Up triangles are results from [25], the diamond symbol is from [39], the star symbol is from [19], the square symbol is from [18] and the down triangle is from [38]. The inset tests the D^{-3} functional fitting for all diameters.

large nanotube diameters, the behaviour can be interpolated very close to a D^{-3} functional form obtained from continuum arguments (here D is the nanotube diameter) [42]. For small nanotube diameters, the D^{-3} relationship fails to reproduce the simulations, which is related to the fact that in this regime the continuum approximation is no longer valid as the nanotube diameter becomes comparable to the carbon–carbon distance. In general, our predictions are in fair agreement with reported experimental results as represented by symbols in the same figure. It is important to mention that these experimental values have been obtained for nanotube bundles and represent an average over a large number of nanotubes with different diameters and chirality. On the other hand, we find a good agreement when comparing our results with those reported in other theoretical calculations, like the one by Capaz *et al* [35].

4. Discussion and conclusions

The study of the properties of isolated carbon nanotubes is becoming of great importance due to the recent developments in producing those nanotubes. On the other hand, there are only few experimental and theoretical results regarding the mechanical and structural properties of isolated SWCNTs under applied pressure. On the theoretical side, Yakobson *et al* [30] and Cornwell and Wille [43] used the Tersoff–Brenner [33] many-body interatomic potential for carbon-made systems for simulations of SWCNTs under generic mechanical loads: axial compression, bending and torsion. Yakobson *et al* found a singular behaviour of the nanotube energy at certain strain levels that corresponds to abrupt changes in morphology, which they explained within a continuous tubule model. Also, Cornwell and Wille [43] found that, under axial compression, nanotubes deform plastically once a certain critical threshold strain is reached, this behaviour being dependent of the tube radii. The cylindrical structure results in different rigidity along different directions of the nanotube. In particular, the axial direction has a high rigidity compared with the radial direction and this property is clearly reflected in the deformation pattern of the nanotubes under pressure. While the nanotube undergoes quite dramatic changes in the radial direction, there is almost no change of the caps.

It is clear from figure 3 (see also figure 2) that upon increasing pressure a single transition, from an oval to a peanut cross-section shape, is observed. The transition pressures obtained from our simulations are in good agreement with recently published results [25]. The rapid transition of the cross-section from the oval one to a peanut starts in the middle of the nanotube and propagates towards the ends. Since our hydrostatic pressure implementation uniformly applies pressure on the whole system, these computational experiments are well suited to calculate the radial compressibility of SWCNTs, which can be directly compared with experimental measurements. We calculated the volume compressibility $\kappa = -\frac{1}{V}\frac{\partial V}{\partial P}$ in the elastic regime at different temperatures for the short (10, 10) nanotube, and found a good agreement with experimental values. We have found a pronounced temperature dependence of κ, in which the compressibility values range from 0.015 to 0.05 GPa^{-1} when T changes from 100 K up to 400 K. The value at $T = 300$ K for short and long (10, 10) tubes is $\kappa = 0.03$ and $\kappa = 0.034$ GPa^{-1}, respectively. These values are in good agreement with the experimental results of $\kappa = 0.024$ GPa^{-1} [19] and $\kappa = 0.028$ GPa^{-1} [5]. Theoretical calculations by Girifalco *et al* [44] assuming a Lennard-Jones potential for the interaction between carbon atoms in a continuum model found the value of $\kappa = 0.022$ GPa^{-1}, and Tersoff and Ruoff [28] by using a similar model found $\kappa = 0.011$ GPa^{-1}, which are also in fair agreement with our results.

From figure 5 we can also conclude that the transition pressure depends only on the diameter of the nanotube and not on its chirality. This agrees with the conclusions of a recent paper [25] in which Elliott *et al* reported that the collapse of SWCNTs under hydrostatic pressure is diameter dependent ($1/D$ for low diameters), and that this collapse does not depend on the nanotube chirality. We found a D^{-3} behaviour of the transition pressure for large nanotube diameters with strong deviations in the case of small diameters, where the elastic theory fails. This observation is in agreement with results published by Elliott *et al* [25] and also agrees with Capaz *et al* [35] at large diameters.

To summarize, in this work we used a surface definition based on Delauney triangulation which provides a fairly good estimation of the surface and volume of the finite system under consideration. The agreement between reported experimental work and our simulations confirms that our methodology is appropriate. The external pressure has been taken into account by applying external forces to the triangulation surface surrounding the structure. The methodology is used to study the behaviour of finite capped SWCNTs under pressure and to characterize the shape changes as a function of pressure. We discuss how these changes depend on the nanotube diameter, chirality and temperature. At small pressures (in the elastic regime), the nanotube response to pressure has been discussed extensively in the literature and we find a fair agreement with those observations. In particular, the dependence of the frequency of the RBM on the diameter is found. Also, we studied the behaviour of some relevant peaks in the power spectra across the structural transitions. With respect to the structural transitions (circular to peanut), we find agreement with previous calculations and experiments but not with the work of Zang *et al* [29]. We find that the transition pressure is diameter dependent, following a D^{-3} decay for large nanotube diameter (as predicted from elastic theory). The transition pressure is also in fair agreement with experimental results for small nanotube diameters where the elastic theory does not hold any more.

Acknowledgments

The authors acknowledge financial support from CONACYT—México through grants J42647-F, J42645-F. Also, SEB is grateful to IPICYT for a PhD scholarship.

References

[1] Mirkin C A, Letsinger R L, Mucic R C and Storhoff J J 1996 *Nature* **382** 607
[2] Star A, Gabriel J-C, Bradley K and Grüner G 2003 *Nano Lett.* **3** 459
[3] ONeal D P, Hirsch L R, Halas N J, Payne J D and West J L 2004 *Cancer Lett.* **209** 171
[4] Cao J, Wang Q and Dai H 2003 *Phys. Rev. Lett.* **90** 157601
[5] Chesnokov S A, Nalimova V A, Rinzler A G, Smalley R E and Fisher J E 1999 *Phys. Rev. Lett.* **82** 343
[6] Andersen H C 1980 *J. Chem. Phys.* **72** 2384
[7] Parrinello M and Rahman A 1980 *Phys. Rev. Lett.* **45** 1196
[8] Martoňák R, Molteni C and Parrinello M 2000 *Phys. Rev. Lett.* **84** 682
[9] Molteni C, Martoňák R and Parrinello M 2001 *J. Chem. Phys.* **114** 5358
[10] Martoňák R, Colombo L, Molteni C and Parrinello M 2002 *J. Chem. Phys.* **117** 11329
[11] Landau A I 2002 *J. Chem. Phys.* **117** 8607
[12] Sun D Y and Gong X G 1998 *Phys. Rev.* B **57** 4730
[13] Calvo F and Doye J P K 2004 *Phys. Rev.* B **69** 125414
[14] Kohanoff J, Caro A and Finnis M W 2005 *ChemPhysChem* **6** 1848
[15] Baltazar S E, Romero A H, Rodríguez-López J L, Terrones H and Martoňák R 2006 Assessment of isobaric–isothermal (*NPT*) simulations for finite systems *Comput. Mater. Sci.* **37** 526
[16] Iijima S 1991 *Nature* **354** 220
[17] Falvo M R, Clary G J, Taylor R M, Chi V, Brooks F P, Washburn S and Superfine R 1997 *Nature* **389** 582
[18] Venkateswaran U D, Rao A M, Richter E, Menon M, Rinzler A, Smalley R E and Eklund P C 1999 *Phys. Rev.* B **59** 10928
[19] Tang J, Qin L, Sasaki T, Yudasaka M, Matsushita A and Iijima S 2000 *Phys. Rev. Lett.* **85** 1887
[20] Gao G, Çagin T and Goddard W A III 1998 *Nanotechnology* **8** 184
[21] Nardelli M B and Bernholc J 1999 *Phys. Rev.* B **60** R16338
[22] Maiti A, Svizhenko A and Anantram M P 2002 *Phys. Rev. Lett.* **88** 126805
[23] Kazaoui S, Minami N, Yamawaki H, Aoki K, Kataura H and Achiba Y 2000 *Phys. Rev.* B **62** 1643
[24] Jiang H, Wu G, Yang X and Dong J 2004 *Phys. Rev.* B **70** 125404
[25] Elliott J A, Sandler J K W, Windle A H, Young R J and Shaffer M S P 2004 *Phys. Rev. Lett.* **92** 095501
[26] Chang S-P, Yim W-L, Gong X G and Liu Z-F 2003 *Phys. Rev.* B **68** 075404
[27] Sluiter M H F, Kumar V and Kawazoe Y 2002 *Phys. Rev.* B **65** 161402
[28] Tersoff J and Ruoff R S 1994 *Phys. Rev. Lett.* **73** 676
[29] Zang J, Treibergs A, Han Y and Liu F 2004 *Phys. Rev. Lett.* **92** 105501
[30] Yakobson B I, Brabec C J and Bernholc J 1996 *Phys. Rev. Lett.* **76** 2511
[31] Harik V M 2001 *Solid State Commun.* **120** 331
[32] Buehler M J, Kong Y and Gao H 2004 *J. Eng. Mater. Technol.* **126** 245
[33] Tersoff J 1986 *Phys. Rev. Lett.* **56** 632
Brenner D 1990 *Phys. Rev.* B **42** 9458
[34] Yamaguchi Y and Maruyama S 1998 *Chem. Phy. Lett.* **286** 336
[35] Capaz R B, Spataru C D, Tangney P, Cohen M L and Louie S G 2004 *Phys. Status Solidi* b **241** 3352
[36] Barber C B, Dobkin D P and Huhdanpaa H 1996 *ACM Trans. Math. Softw.* **22** 469
[37] Hughes S W, D'Arcy T J, Maxwell D J, Saunders J E, Ruff C F, Chiu W S C and Sheppard R J 1996 *Phys. Med. Biol.* **41** 1809
[38] Peters M, McNeil L E, Lu J P and Khan D 2000 *Phys. Rev.* B **61** 5939
[39] Sandler J, Shaffer M S P, Windle A H, Halsall M P, Montes-Morán M A, Cooper C A and Young R J 2003 *Phys. Rev.* B **67** 035417
[40] Venkateswaran U D, Masica D L, Sumanasekera G U, Furtado C A, Kim U J and Eklund P C 2003 *Phys. Rev.* B **68** 241406(R)
[41] Kürti J, Kresse G and Kuzmany H 1998 *Phys. Rev.* B **58** R8869
[42] Lévy M 1884 *J. Math. Pures Appl.* **10** 5
[43] Cornwell C F and Wille L T 1998 *Comput. Mater. Sci.* **10** 42
[44] Girifalco L A, Hodak M and Lee R S 2000 *Phys. Rev.* B **62** 13104